主　論　文

Transport anomalies and suppression of superconductivity in $La_{2-x-y}Nd_yBa_xCuO_4$

Xiuzeng Bao

Department of Physics, Faculty of Science, Hiroshima University,
Higashi-Hiroshima 739, Japan

(January, 1997)

Contents

Abstract

It is well known that a striking suppression of superconductivity of $La_{2-x}Ba_xCuO_4$ occurs in a narrow range of x around 1/8, accompanied by a structural phase transition from a mid-temperature orthorhombic (OMT) phase to a low-temperature tetragonal (TLT) phase below about 60 K. It seems that the suppression of superconductivity requires both a Ba concentration of x=1/8 and a distortion of the lattice from the OMT phase to the TLT phase. For the first condition, partial replacement of La^{3+} by Th^{4+} ($La_{2-x-y}Th_yBa_xCuO_4$) clearly reveals that the hole concentration of $p=x-y=1/8$ per Cu is of essential importance to the suppression of superconductivity, instead of Ba concentration of x=1/8. For the second condition, however, it is not clear to date what specific role the structural phase transition plays in the severe suppression of T_c around p=1/8. The purpose of this study is to help clarify what role the structural phase transition plays and what relationship there exists among the anomalies of transport properties, the structural phase transitions and the suppression of superconductivity around x=1/8.

The interplay among transport properties, structural phase transitions and superconductivity in $La_{2-x-y}Nd_yBa_xCuO_4$ has been studied. We found that the temperature at which the thermopower $S(T)$ begins to show unusual decrease on cooling coincides with that of the minimum in the resistivity for the samples with x around 1/8. Moreover, the appearance of negative thermopower accompanies the suppression of superconductivity. However, we did not find any anomaly in the thermopower and in the resistivity at the structural phase transition temperature T_{d2} for any of the samples in this study. The results show that in this series of compounds, the suppression of superconductivity around x=1/8 is not directly associated with the structural phase transition but with the profound change of the transport properties.

1. Introduction

It is well known that the curious disappearance of bulk superconductivity of $La_{2-x}Ba_xCuO_4$ (LBCO) occurs in a narrow range of x around 1/8 [1] accompanied by a structural phase transition from a mid-temperature orthorhombic (OMT) phase [2] with space group Bmab to a low-temperature tetragonal (TLT) phase with space group $P4_2/ncm$ below about 60 K [3-6]. It was believed that the suppression of superconductivity requires both a Ba concentration of x=1/8 and a distortion of the lattice from the OMT phase to the TLT phase. The origin of the suppression of superconductivity in the narrow range of x around 1/8, which is called the 1/8 problem, has attracted considerable interest. It is hoped that the clarification of this anomaly will give a clue to the mechanism of superconductivity in high-T_c cuprates.

In order to investigate the origin of the anomalies and the relationship between the structural phase transition and the striking suppression of superconductivity, we have previously studied two series of samples of $La_{2-x-y}Th_yBa_xCuO_4$ (LTBCO): the one has a fixed value of y (y=0.020) and varied values of x ($0.007 \le x \le 0.170$) [7,8] and the other has a fixed value of x (x=0.145) and varied values of y ($0 \le y \le 0.04$)[9]. For the first series of samples the center of sharp depression of T_c, as well as of the structural phase transition, shifts from x=1/8 for LBCO to x=0.145 for LTBCO with y=0.020 [shown in Fig.1(a)]. For the second series of samples the TLT phase is most stable at y=0.020 and the striking suppression of superconductivity is also centered at y=0.020 [shown in Fig.1(b)]. The partial replacement of trivalent ions La^{3+} by quadrivalent ions Th^{4+} ($La_{2-x-y}Th_yBa_xCuO_4$) clearly reveals that the suppression of superconductivity is centered at x=1/8+y rather than at x=1/8. The same conclusion has been drawn by study of substitution with other rare earth element [10]. On the other hand, with partial replacement of La^{3+} by trivalent ions R^{3+} ($La_{2-x-y}R_yBa_xCuO_4$, R=Gd, Dy) [11], the minimum of T_c is still at x=1/8. These substitute studies of different valent ions for La^{3+} indicate that a particular value for the concentration of holes per Cu, p=1/8, is of essential importance to the suppression of superconductivity, instead of Ba concentration

of x=1/8.

For the second condition, many efforts [12–16] have been made which focus on the effects of the structural phase transitions at low temperatures on the suppression of superconductivity. However, it is not clear to date what specific role the structural phase transition plays in the severe suppression of T_c around p=1/8. The previous studies on the element substitution effects for Ba in LBCO [6,16] show a strong correlation between the lattice instability and electronic properties. The disappearance of the TLT phase is correlated with the recovery of T_c in the Ba–site substituted systems ($La_{2-x}Ba_{x-y}M_yCuO_4$, M=Sr and Ca). Nevertheless, in high pressure studies of LBCO around x=1/8 [17,18], T_c increases until the TLT phase is completely suppressed by pressure. However even at the pressure of 20 kbar at which the TLT phase is suppressed [18], the reduction in T_c is still evident at x=1/8 [17]. It therefor seems that the structural phase transition is not the direct origin of the suppression of T_c near p=1/8. The purpose of this study is to help clarify what role the structural phase transition plays and what relationship there exists among the anomalies of transport properties, the structural phase transitions and the suppression of superconductivity around x=1/8.

Because Nd is stable only as trivalent ions in oxides and has a smaller ionic radius than La, the substitution for La^{3+} by Nd^{3+} will not change the density of holes but will change the crystal structure even for the samples with the same Ba concentration. Therefore we can readily control the hole density p and the structural phase transition temperatures by changing Ba concentration x and Nd concentration y, respectively. In the present study we have studied two series of polycrystalline samples of $La_{2-x-y}Nd_yBa_xCuO_4$ (LNBCO). For the first series of samples we have chosen the fixed value x(Ba)=1/8 to investigate the effects of Nd doping in LBCO on the structural phase transition, transport properties and superconductivity at x=1/8. For the second series of samples we have chosen the fixed value y(Nd)=0.20 because this value changes T_{d2} substantially without destructing superconductivity severely. The interplay among the transport properties, superconductivity and structural phase transitions was investigated by electrical resistivity, thermoelectric power, diamagnetic susceptibility, low–temperature powder X–ray diffraction, and ultrasonic velocity measurements.

Our previous study [19] indicated that the structural phase transition temperature T_{d2} (OMT–TLT) is enhanced by 50K by partial substitution of Nd with y=0.20 in LBCO with x=1/8. A subsequent study of transport properties indicated no anomalous behavior at T_{d2} [20]. The present results show further that the unusual decrease of thermopower on cooling occurs just below the temperature (we call T_{min}) at which the resistivity takes the minimum. The suppression of superconductivity is connected with the appearance of negative thermopower. There is no evidence that a structural phase transition occurs at about the temperature T_{min} by X–ray diffraction as well as by ultrasonic velocity measurement. Conversely we do not find any anomaly of the transport properties at about T_{d2}. These mean that the suppression of superconductivity for LNBCO with x around 1/8 is not directly related with the structural phase transition but is caused by the instability of the electronic state.

In Section 2 of this thesis we present the sample preparation and the measurement methods. We also give a brief description about the homemade experimental setup for the thermopower measurement. In Section 3 we show the experimental results of various measurements. In Section 4 we discuss the experimental results and propose a simple phenomenological density–of–states model to describe the origin of the negative thermopower. Finally in Section 5 we give our conclusion.

2. Experimental procedure

2.1 Sample preparation

In this study two series of polycrystalline samples of $La_{2-x-y}Nd_yBa_xCuO_4$ (LNBCO) were prepared: the one has a fixed value of x (x=1/8) and varied values of y ($0 \leq y \leq 0.60$: y=0, 0.05, 0.10, 0.20, 0.40, 0.60) and the other has a fixed value of y (y=0.20) and varied values of x ($0 \leq x \leq 0.250$: x=0, 0.02, 0.04, 0.06, 0.075, 0.100, 0.110, 0.120, 0.125, 0.130, 0.140, 0.150, 0.160, 0.170, 0.175, 0.190, 0.200, 0.210, 0.225, 0.250). In order to make a comparison between LNBCO and LBCO, we also prepared two polycrystalline samples of $La_{2-x}Ba_xCuO_4$ with x=0.14 and x=0.16. The polycrystalline samples were prepared by solid-state reaction from appropriate mixtures of dried powders of La_2O_3, $BaCO_3$, CuO and Nd_2O_3 in stoichiometric ratio. Each of these powders has a purity of 99.99%. The powders were mixed, pelletized, and reacted at 1000 °C in air for 24 hours. Then the pellets were reground, pelletized, and reacted at 1050 °C for 24 hours. This procedure was repeated again but reacted at a slightly higher temperature of 1100 °C. Finally, the pellets were annealed in flowing oxygen at 500 °C for 96 hours to minimize oxygen deficiencies. The samples were confirmed to be of single phase by powder X-ray diffraction.

Each of the annealed samples has a weight of about 10g with a diameter of about 20mm and a thickness of about 8mm. The samples were then cut with a diamond saw. The dimensions of the cut samples are approximately $1.0 \times 2.0 \times 12.0$ mm^3, $1.0 \times 1.5 \times 10.0$ mm^3 and $2.0 \times 3.0 \times 4.5$ mm^3 for resistivity, thermopower and ultrasonic velocity measurements, respectively. For low-temperature X-ray diffraction and diamagnetic susceptibility measurements, the samples were ground into powder with weights of about 300mg and 400mg, respectively.

2.2 Measurement methods

To investigate the structural phase transitions, we performed powder X-ray diffraction in a wide temperature range from room temperature down to 5K using a

flow-type ^{4}He cryostat. To determine the superconducting transition temperature, we measured diamagnetic susceptibility by a SQUID magnetometer on cooling in a field of 3.0 Oe. Electrical resistivity was measured by an ordinary four-probe method with a constant current of 10mA. Thermopower was measured by a conventional method with a homemade apparatus. We have controlled the temperature gradient at 1.4K/8mm in the entire temperature range from room temperature down to 5K for every thermopower measurement. The linearity of the measured thermal electromotive force with respect to the temperature gradient was carefully checked.

For a sensitive detection of a possible structural phase change at T_{min}, We have also measured the ultrasonic velocity for $La_{1.68}Nd_{0.20}Ba_{0.12}CuO_4$ at a frequency of 17 MHz.

2.3 Experimental set up for the thermopower measurement

As is well known, a temperature gradient over a metal sample will give a voltage difference from the cold end to the hot end of the metal sample. Thermopower is defined as the thermo electromotive force per unit increment in temperature. As is shown in Fig.2, we can determine the thermopower of the sample S_S by measuring the voltages V_1 and V_2. V_1 can be expressed as

$$V_1 = -\int_{T_1}^{T_0} S_A dT - \int_{T_0}^{T_0+\Delta T} S_S dT - \int_{T_0+\Delta T}^{T_1} S_A dT , \qquad (1)$$

where S_A is the thermopower of the copper lead at a given temperature and S_S is that of the sample. Then,

$$V_1 = \int_{T_0}^{T_0+\Delta T} (S_A - S_S) dT . \qquad (2)$$

This gives to a good accuracy

$$V_1 = (S_A - S_S) \cdot \Delta T , \tag{3}$$

in which S_A and S_S are the values at $T = T_0 + \Delta T_0/2$. In the same way,

$$V_2 = (S_B - S_S) \cdot \Delta T , \tag{4}$$

where S_B is the thermopower of the alloy constantan lead. Combine Eq.3 with Eq.4,

$$\Delta T = \frac{V_1 - V_2}{S_{AB}} , \tag{5}$$

where $S_{AB}=S_A-S_B$. From Eq.3 the thermopower of the sample can be expressed as

$$S_S = S_A - \frac{V_1}{\Delta T} . \tag{6}$$

With Eq.5, we express Eq.6 as

$$S_S = S_A - \frac{V_1}{V_1 - V_2} \cdot S_{AB} . \tag{7}$$

Eq.7 is the fundamental equation which we used to calculated the thermopower of the samples in this study. We have used the values of the international industrial standards

for the relative thermopower S_{AB} [21]. The absolute thermopower of the copper lead S_A was given by reference 22. Because at lower temperatures the absolute thermopower of copper is very sensitive to impurities and defects of specific material used, we have calibrated S_A below 50K by using a superconducting sample of YBCO. As S_{AB} and S_A are known the thermopower of the sample S_S is obtained by measuring V_1 and V_2.

The experimental setup for the measurement of thermopower is shown schematically in Fig.3 and the sample holder was depicted in Fig.4. As shown in Fig.4, the sample is attached between two copper blocks: the cold block and the hot block. The two blocks are linked up by a brass bolt with the thermal conductance low enough to establish the temperature gradient but high enough compared with that of the sample. Thus the heat will flow mainly through the brass bolt and the thermal resistance between the two copper blocks will not be affected by the size or the shape of the samples. Two pairs of thermocouples were connected to the sample. We have used thermocouple pairs of type T (copper and constantan). This thermocouple can be used in the temperature range from 3K to 673K. Two heaters are attached to the two copper blocks. The main heater on the cold block is used to establish the system temperature (T). The sub heater on the hot block is used to establish a temperature gradient in the sample by heating the hot block to a higher temperature ($T+\Delta T$). Two resistance thermometers in the cold block are used to measure the system temperature. One is the platinum resistance thermometer (PRT) which is used at higher temperatures (T>50K); the other is the germanium resistance thermometer (GRT) which is used at lower temperatures (T<55K).

The sample holder is mounted in a vacuum can. After the sample is set up, the vacuum is pumped to a typical pressure of 4×10^{-6} Torr. This high vacuum is needed to hold a stable temperature inside the vacuum can. Then the vacuum can is put into a double glass dewar. In the outside dewar we fill liquid nitrogen and in the inner dewar liquid helium. Between the two liquids there exists a vacuum space which is used to prevent the helium to boil off too fast. By the DC current supplies (as shown in Fig.3), through the Temperature Controller we can control the system temperature at any given temperature (from 5K to room temperature) with an appropriate temperature gradient (in our experiment we let $\Delta T/\Delta l$ = 1.4K/8mm). After the system temperature becomes stable,

we measure V_1 and V_2 by the DMM. A micro-computer is used to evaluate ΔT, S_A, S_{AB} and S_S, and the data for T, V_1, V_2, ΔT, S_A, S_{AB} and S_S are stored into a disc and printed out by a printer at the same time.

3. Experimental Results

3.1 Results for $La_{2-x-y}Nd_yBa_xCuO_4$ (x=1/8, $0 \le y \le 0.60$)

Powder X-ray diffraction study at low temperatures revealed that with any Nd concentration investigated in this study $La_{1.875-y}Nd_yBa_{0.125}CuO_4$ ($0 \le y \le 0.60$) undergoes the same sequence of structural phase transitions as $La_{1.875}Ba_{0.125}CuO_4$. Figure.5(a) shows a part of the powder X-ray diffraction spectra at some selected temperatures for y=0.20 and x=1/8. As temperature decreases the structure first transforms from a high-temperature tetragonal (THT) phase to the OMT phase at the temperature T_{d1} and then transforms to the TLT phase at some lower temperature T_{d2}. In this study we define T_{d2} as the temperature at which the ratio of the integrated intensity of the TLT peaks to the total peak intensity becomes 50%. The former transition (THT-OMT) is of the second order, whereas the latter transition (OMT-TLT) is of the first order. As shown in Fig.5(a), at 300K there exists only one peak which is (220) diffraction peak of the THT phase. With decreasing temperature it transforms to two peaks which are (040) and (400) peaks of the OMT phase. At 150K these two peaks are clearly visible. Below 130K a new peak, the (400) peak of the TLT phase, appears between these two peaks. It grows with the expense of the intensities of the OMT peaks as temperature decreases. The OMT peaks in our samples did not disappear entirely even at 5K, but their intensity was less than 16% of the total peak intensity.

Nd concentration dependence of T_{d1} and T_{d2} is plotted in Fig.6. As shown, both T_{d1} and T_{d2} increase substantially with increasing Nd concentration y. With increasing Nd concentration, T_{d2} increases from 65K (y=0) up to 135K (y=0.60) for the same hole concentration of p=1/8, although it tends to saturate at higher values of y.

Diamagnetic susceptibility of the powdered samples of $La_{2-x-y}Nd_yBa_xCuO_4$ (x=1/8) on cooling in a field of 3.0 Oe is shown in Fig.7. Only a weak diamagnetism is perceived for small Nd concentrations. With increasing y, the diamagnetism becomes unnoticeable and Curie-like behavior due to the localized moment of Nd^{3+} becomes appreciable. After subtracting the latter contribution using measured paramagnetic

susceptibility at 10 kOe, we estimate the diamagnetic contribution to be at most about 1% of the volume fraction for any y.

Fig.8 shows the temperature dependence of the resistivity, showing a distinctive upturn of the resistivity below T_{min}=60–70K. With decreasing temperature a two–step superconducting transition was observed. The higher one, a small negative step at about 30 K, is most likely due to the filamentary part of the specimen. The lower one, a gradual decrease toward zero below 10 K, may indicate the intrinsic superconducting transition. However it is weak superconductivity as probed by the flux expulsion measurements (at most 1% volume fraction of perfect diamagnetism). Above T_{min} the resistivity shows the metal properties. We did not found any anomaly in the resistivity at T_{d2} for all the samples as shown in Fig.8.

The variation of the thermopower $S(T)$ is shown in Fig.9. The overall temperature dependence is not much affected by the change in Nd concentration y. It shows only a small decrease in the magnitude with increasing y. At higher temperatures the thermopower first increases slowly with decreasing temperature and then decreases slowly with further decreasing temperature below about 150–200K. Below T=60–70K (which we call T^* in this study), S begins to fall down sharply, crosses zero rapidly, attains the largest negative value at about 25K and then returns toward zero as the temperature approaches zero.

We summarized the Nd concentration dependence of T_{d2}, T_{min} and T^* in Fig.10. As shown, T_{d2} increase substantially with increasing Nd concentration y. With increasing Nd concentration, T_{d2} increases from 65K (y=0) up to 135K (y=0.60) for the same hole concentration of p=1/8. In contrast, T_{min} and T^* show a much weaker y dependence than T_{d2}. At lower Nd concentration (near y=0), the values of T_{min}, T^* and T_{d2} are nearly the same. With increasing Nd concentration, T_{min} and T^* agree with each other but T_{d2} becomes larger than T_{min} and T^* by about 60K for the sample with y=0.40. It should be noted that T_{d2} coincides with T_{min} and T^* in LBCO without Nd (y=0), suggesting that the interplay between structural phase transition and charge instability becomes important only in the immediate vicinity of that composition.

3.2 Results for $La_{2-x-y}Nd_yBa_xCuO_4$ (y=0.20, $0 \leq x \leq 0.25$)

Low-temperature power X-ray diffraction study revealed that the samples with higher Ba concentration ($x \geq 0.10$, y=0.20) undergoes the same sequence of structural phase transition as $La_{1.875}Ba_{0.125}CuO_4$ as described in Section 3.1. For the samples with lower Ba concentration (x<0.10, y=0.20) another first order structural phase transition, from the OMT phase to the low-temperature orthorhombic (OLT) phase consistent with space group Pccn, was observed. This transition is shown in Fig.5(b) with a part of the powder X-ray diffraction spectra at selected temperatures for y=0.20 and x=0.075. At 300K the existing two peaks are (040) and (400) diffraction peaks of the OMT phase. Below 100K two new peaks of the OLT phase appear between the (040) and (400) peaks of the OMT phase. These four peaks coexist down to 5K.

Ba-concentration dependence of T_{d1} and T_{d2} for $La_{2-x-y}Nd_yBa_xCuO_4$ (y=0.20, $0 \leq x \leq 0.25$) is plotted in Fig.11. Compared with Nd-free LBCO, for which structural phase transition (OMT-TLT) occurs only in a narrow range of x around 1/8, the Nd-substituted system has higher values of T_{d1} and T_{d2} for the same Ba concentration and exhibits the structural phase transition (OMT-TLT) in a wider range of x ($0.100 \leq x \leq 0.200$).

Temperature dependence of the magnetic susceptibilities for these samples are shown in Fig.12. The Ba concentration dependence of T_c and the magnetic susceptibility at 5K are summarized in Fig.13. Here we define T_c as the temperature at which the sample exhibits 1% volume fraction of perfect diamagnetism. As shown in Figs.12 and 13, the suppression of superconductivity is not restricted in the immediate vicinity of x=1/8 but spreads over somewhat wider range of x ($0.120 \leq x \leq 0.140$).

The temperature dependence of the thermopower is shown in Fig.14. At higher temperatures the thermopower $S(T)$ decreases systematically with increasing Ba concentration x, and increases slowly with decreasing temperature for given x. At lower temperatures $S(T)$ approaches zero in three kinds of ways depending on x as shown in Fig.15. For the overdoped samples, such as the one with x=0.25, $S(T)$ decreases slowly with decreasing temperature and monotonically approaches zero at T=0. For the

superconductors, for example with x=0.190, S (T) begins to fall down sharply at some temperature slightly above T_c and drops down to zero in the superconducting state. For the samples with x around 1/8 ($0.120 \leq x \leq 0.140$), for which the superconductivity is suppressed, $S(T)$ begins to fall down sharply at the temperature T^*, crosses zero rapidly, attains the largest negative value and then return toward zero as the temperature approaches zero.

Fig.16 shows the relationship between the anomaly of resistivity and that of thermopower. Ba concentration dependence of T_c, T_{d2}, T_{min} and T^* was summarized in Fig.17. For the same Ba concentration, the values of T_{min} and T^* are nearly the same but the value of T_{d2} is about 50K higher than those of T_{min} and T^*; the thermopower begins to drop at the temperature of minimum in resistivity. It is also evident from Fig.16 that there is no anomaly at T_{d2} either in the resistivity or in the thermoelectric power at least for the polycrystalline samples.

Moreover, as we already noted above, the suppression of superconductivity not only occurs at x=1/8 but spreads over somewhat wider range of x ($0.120 \leq x \leq 0.140$). The disappearance of superconductivity at x=0.140 is caused by the introduction of Nd which induces the structural phase transition (OMT–TLT), indicating that the TLT phase is not favorable to superconductivity. Nevertheless the TLT phase itself is not the direct origin of the severe suppression of superconductivity around x=1/8. As shown in Figs.13 and 17, bulk superconductivity exists under the TLT phase for the samples with x far away from 1/8. Among them, at x=0.100 and x=0.170, the volume fractions of perfect diamagnetism are higher than 16% at 5K even on powdered samples.

As a sensitive probe of a possible structural phase change at T_{min}, we have also measured the ultrasonic velocity for $La_{1.68}Nd_{0.20}Ba_{0.12}CuO_4$. As shown in Fig.18 obvious hardening is observed at about 125K, which is the response to the structural phase transition (OMT–TLT). This temperature is consistent with T_{d2} (onset) determined by powder X–ray diffraction. At T_{min} and T^*, however, we did not find any anomaly in the T–dependence of the ultrasonic velocity. Therefore there is no evidence for additional structural phase transition at the temperatures of T_{min} and T^*.

3.3 Comparison between LNBCO and LBCO

To compare with LBCO let us now focus on samples with x=0.140 and x=0.160. The results are shown in Fig.19. For the same Ba concentration of x, compared with LBCO (y=0), a visible difference $S(T)$ appears only at lower temperatures connected with the difference in superconducting properties. At x=0.140 for the sample of LNBCO (T_c<4K) $S(T)$ becomes negative below 30K associated with the suppression of superconductivity. But for the sample of LBCO (T_c=25K) such negative S does not appear. At x=0.160 $S(T)$ of both samples are similar, reflecting that the samples with y=0 and y=0.20 are both superconductors with T_c=28K and 18K, respectively. As we have shown in Section 3.1 negative $S(T)$ also appears for the samples of $La_{2-x-y}Nd_yBa_xCuO_4$ (x=1/8, $0 \le y \le 0.60$) for which superconductivity is suppressed. Similar phenomenon of negative thermopower was also observed in the rare earth doped LSCO ($La_{2-x-y}R_ySr_xCuO_4$) associated with the suppression of superconductivity [23]. It is important to note in Fig.19 that although T_{d2} is very different between LBCO and LNBCO for the same value of x, we did not find any anomaly in the thermopower at T_{d2} for these four polycrystalline samples. Rather, it is clear that the suppression of superconductivity has some relation with the appearance of the negative values of thermopower.

4. Discussion

4.1 Structural phase transition and transport properties

In the samples of $La_{2-x-y}Nd_yBa_xCuO_4$ (x=1/8, $0 \le y \le 0.60$) the structural phase transition (OMT–TLT) temperature T_{d2} increases substantially with increasing Nd concentration y. As we have shown, with increasing Nd concentration, T_{d2} increases from 65K (y=0) up to 135K (y=0.60) for the same hole concentration of p=1/8. In contrast, T_{min} and T^* show a much weaker y dependence than T_{d2}. At lower Nd concentration (near y=0), the values of T_{min}, T^* and T_{d2} are nearly the same. With increasing Nd concentration, T_{min} and T^* agree with each other but T_{d2} becomes larger than T_{min} and T^* by about 60K for the sample with y=0.40 (shown in Fig. 10). For the samples of $La_{2-x-y}Nd_yBa_xCuO_4$ (y=0.20, $0.120 \le x \le 0.140$) with a given Ba concentration, the values of T_{min} and T^* are nearly the same (60–70K) but the value of T_{d2} is about 50K higher than those of T_{min} and T^* (shown in Fig.17). It is clear that the anomalies of the transport properties and the structural phase transition occur at different temperatures and that there is no anomaly at T_{d2} neither in the resistivity nor in the thermopower for the samples with higher Nd concentration. This seems that there is no direct relation between the anomalies of the transport properties and the structural phase transition. It should be noted that T_{d2} coincides with T^* in LBCO without Nd (y=0), suggesting that the interplay between structural phase transition and charge instability becomes important only in the immediate vicinity of that composition. One the other hand it is noticed that the anomalies of transport properties, such as the minimum of resistivity and the negative thermopower, are observed only in the TLT phase for the samples in our study. Therefore the TLT phase seems to be a necessary condition for the anomalies of the transport properties to appear.

4.2 Structural phase transition and superconductivity

As we have already noted above, compared with Nd-free LBCO, for which structural phase transition (OMT–TLT) and suppression of superconductivity occur only

in a narrow range of x around 1/8, the Nd-substituted system exhibits the structural phase transition (OMT-TLT) in a wider range of x ($0.100 \leq x \leq 0.200$) and the suppression of superconductivity not only occurs at x=1/8 but spreads over somewhat wider range of x ($0.120 \leq x \leq 0.140$). The disappearance of superconductivity at x=0.140 is caused by the introduction of Nd which induces the structural phase transition (OMT-TLT), indicating that the TLT phase is not favorable to superconductivity. Nevertheless the TLT phase itself is not the direct origin of the severe suppression of superconductivity around x=1/8. As shown in Figs.13 and 17, bulk superconductivity exists even under the TLT phase for the samples with x far away from 1/8. Moreover, as we have mentioned in Section 1, in high pressure studies of LBCO around x=1/8 [17,18], T_c increases until the TLT phase is completely suppressed by pressure. However even at the pressure of 20 kbar at which the TLT phase is suppressed [18], the reduction in T_c is still evident at x=1/8 [17].

4.3 Transport properties and the suppression of superconductivity

We have demonstrated that there is no direct relation between the anomalies of the transport properties and the structural phase transition. In contrast, there exists a definite relation between the anomaly of the resistivity and that of the thermopower. The sharp change in $S(T)$ coincides clearly with the minimum of the resistivity for the samples with x around 1/8: when the resistivity takes the minimum, the thermopower begins to drop and become negative at lower temperatures.

We argue that the anomalies of the transport properties are caused by charge localization. Charge localization is clearly recognized in the transport properties: at T_{min} the sample changes from metallic to nonmetallic behavior; the thermopower begins to drop sharply below T^* and becomes negative at lower temperatures for the samples with x around 1/8. This behavior of the thermopower is attributed to the development of a gap-like structure in the density of states. We will discuss below that the sharp decrease in the thermopower starting at T^* is consistent with the charge localization.

As shown in Fig.14, thermopower decreases systematically with increasing Ba concentration at higher temperatures but changes drastically at lower temperatures. We

plotted the Ba concentration dependence of the thermopower in Fig.20 at several selected temperatures. At higher temperatures all of the samples have positive values of $S(T)$. At lower temperatures negative $S(T)$ appears for the samples with x around 1/8 as shown in Fig.20 for 30K and 10K.

For a sufficiently pure metal the thermopower $S(T)$ is approximately linear in temperature and shows a narrow phonon drag peak at lower temperatures [22,24]. This phonon drag thermopower is often diminished by impurities. But for high-T_c cuprates the thermopower is more complicated than that of a usual metal. In general, the thermopower of high-T_c cuprates decreases with increasing hole concentration p; $S(p)$ is positive for lightly doped materials and negative for highly over-doped materials. The details of T dependence are quite different among different high-T_c cuprates. For LBCO system, as mentioned above, $S(T)$ shows a strong and broad peak at high temperatures. This behavior of the thermopower has also been reported for other materials based on La_2CuO_4 [20,23,25-34]. For $YBa_2Cu_3O_7$ system [29,32,35-47], $S(T)$ shows a weaker temperature-linear dependence and takes negative values for the samples with high hole concentration. For $Bi_2Sr_2CaCu_2O_8$ system [43,45,46], $S(T)$ contains a term which varies linearly with temperature with a large negative slope. Before discussing the negative thermopower of LNBCO let us first briefly review how the thermopower of high-T_c cuprates has been interpreted.

Because the basic physics of high-T_c cuprates is described by the Hubbard model, it is natural to interpret the experimental results using the predictions of the Hubbard model for the thermopower which considers correlated hopping [26,28]. In the high-temperature limit, if k_BT is greater than the bandwidth W but much less than the on-site Coulomb repulsion U, the thermopower is expressed [48,49] as:

$$S = -\frac{k_B}{|e|}\left(\ln 2 + \ln\frac{p}{1-p}\right), \qquad (8)$$

where p is the number of hole per Cu site. The ln2 term comes from the spin degree of

freedom and is absent if Cu^{2+} ions order magnetically such as in pure La_2CuO_4. According to Eq.8, S decreases as p increases but remains positive as long as $p<1/3$. This is at least consistent with the experimental result that the thermopower decreases with the increase of hole doping, although the condition of k_BT greater than W is not satisfied for the cuprates. According to Eq.(8) the thermopower has a contribution from spin entropy which should be quenched by a large magnetic field. Yu et al. [29] reported that in studying the effect of the large magnetic field on the thermopower for YBCO their experimental results, however, show a field independent thermopower up to 30T. There seems to be some problems to apply this theory to high-T_c cuprates.

Kang et al. [42] proposed the magnon-drag effect on the thermopower. They suggested that even in superconducting samples the presence of antiferomagnetic fluctuations gives rise to an extra contribution to the thermopower as a result of interaction with electrons. However, the experimental confirmation needs to be made. The magnon-drag thermopower has a similar expression to that of the phonon-drag thermopower except that the phonon specific heat is replaced by magnetic specific heat.

Trodahl [50] has tried to interpret the complex T dependence of the thermopower of high-T_c cuprates by a model in which the total thermopower (S_{net}) consists of two contributions: one is the diffusion thermopower (S_d) which is proportional to temperature and has a negative value, and the other is the phonon drag thermopower (S_g) which depends only weakly on temperature and has a positive value. He argued that because the phonon-phonon scattering remains weaker than phonon-electron scattering up to 300K, the phonon drag thermopower is strong even at room temperature. The phonon drag thermopower S_g consists of positive and negative contribution, depending on the relative

direction of the velocity change of the electron with respect to the phonon velocity. The balance between the two contributions is controlled by the hole doping. As hole concentration is raised negative contribution increases and the total S_g decreases. This model seems to reproduce reasonably the experimental results of thermopower of high-T_c cuprates.

If such a term is assumed for our experimental results shown in Fig.14, S_{net} is

mainly decided by S_g for all of the samples in this study at high temperatures ($T>T^*$) and also for the samples with x not around 1/8 at low temperatures because S_{net} is positive or zero (in superconducting state). But for the samples with x around 1/8 at lower temperatures ($T<T^*$) S_{net} takes negative values, showing that S_{net} is decided mainly by S_d. The diffusion thermopower can be expressed by the Mott formula [22,24]:

$$S_d = -\frac{\pi^2 k_B^2 T}{3|e|\sigma(\varepsilon_F)}\left[\frac{\partial\sigma(\varepsilon)}{\partial\varepsilon}\right]_{\varepsilon=\varepsilon_F}, \qquad (9)$$

where k_B is Boltzman's constant, $|e|$ is the elementary charge, and $\sigma(\varepsilon)$ is the hypothetical conductivity for the Fermi level at ε. Using a well known expression of $\sigma(\varepsilon_F)$ for the isotropic three dimensional case

$$\sigma(\varepsilon_F) = \frac{2}{3}e^2 v_F^2 \tau N(\varepsilon_F), \qquad (10)$$

we express Eq.(9) as

$$S_d = -\frac{\pi^2 k_B^2 T}{3|e|}\left[\frac{1}{N(\varepsilon_F)}\frac{\partial N(\varepsilon)}{\partial\varepsilon} + \frac{1}{v_F^2\tau}\frac{\partial(v_F^2\tau)}{\partial\varepsilon}\right]_{\varepsilon=\varepsilon_F}. \qquad (11)$$

Here v_F is the Fermi velocity, τ is quasiparticle life time and $N(\varepsilon_F)$ is the density of states at the Fermi level. In this expression, we argue that the first term plays a key role in the appearance of negative $S(T)$ at lower temperatures for the samples with x around 1/8. In order to describe the origin of the negative thermopower, we consider a simple phenomenological density-of-states model as sketched in Fig.21, in which it is assumed that the Fermi level ε_F shifts by doping. Such a model is in fact supported by the results

of ultrasonic measurements on single crystals of LSCO [51]. At higher temperatures ($T>T^*$) as shown in Fig.21(a), the density of states at the Fermi level decreases with increasing ε_F. According to Eq.(11), a negative energy-derivative of the density of states will give a positive contribution to the diffusion thermopower. The first term will give a positive contribution and this contribution will decrease with increasing hole doping; but the total diffusion thermopower is negative. At lower temperatures ($T<T^*$) as shown in Fig. 21(b), for the samples around x=1/8 the density of states splits into two peaks, reflecting the formation of a gap due to the charge localization. The formation of the gap-like structure may lead to a positive energy derivative of the density of states at the Fermi level, to support the observed large negative contribution to thermopower according to Eq.(11). We believe that this is the main reason that thermopower take negative values for the samples with x around 1/8. The energy dependence of τ and v_F may also give substantial effects on the appearance of the negative thermopower and further theoretical work is needed.

We have shown that the suppression of superconductivity around x=1/8 is directly associated with the sharp change of the transport properties. This change is likely caused by the localization of the electrons near the Fermi level. It is important to note that this change occurs below about 70K, which is about 50K lower than the structural phase transition temperature T_{d2}. This means that the suppression of superconductivity is caused by the instability of the electronic states near the Fermi level. This result is consistent with the formation of charge order as suggested by recent electron diffraction [52] as well as neutron diffraction [53] studies.

In the electron diffraction experiment for the sample LNBCO with y=0.20 and x=1/8, Ito et al. [52] observed the [1/2 1/2 0] type superlattice below 70K showing the formation of charge order, whereas they observed that the transition temperature T_{d2} is about 110K for that sample. These values well correspond to T^* and T_{d2}, respectively in the present study.

Similar superlattice was observed in $La_{2-x-y}Nd_ySr_xCuO_4$ with x=0.12 and y=0.40 by neutron diffraction [53]. Tranquada et al. reported that they observed two kinds of superlattice peaks below 70K: spin-related and charge-related peaks. That experiment

gives a suggestion that there exists a static ordered stripe of charge and spin at low temperatures in this compound. The ordered charge stripe has a period of $4a$, four times larger than that of the lattice parameter a. This causes the appearance of an energy gap at $\pi/4a$ in the reciprocal lattice, leading to the suppression of the superconductivity. Although the atomic displacements in the TLT phase seem to be favorable to the observed superlattice associated with the charge ordering [53], we still do not fully understand why the charge localization occurs only in the TLT phase.

5. conclusion

By our experiment, we conclude that the structural phase transition (OMT–TLT) itself is not the direct origin of the suppression of superconductivity in LNBCO around p=1/8, although the TLT phase is not favorable to superconductivity. In contrast, the suppression of superconductivity in LNBCO around p=1/8 is directly associated with the sharp change of the normal–state transport properties. The anomalies of the transport properties are attributed to the charge localization. This means the suppression of superconductivity is caused by the instability of the electronic states near the Fermi level at temperatures lower than T_{d2} for the structural phase transition (OMT–TLT).

Let us summarize a scenario for the suppression of superconductivity for x around 1/8. As the temperature decreases below T_{min}, the electrons begin to localize and the charge order is formed. The density of states split into two peaks and the gap–like structure is produced. The sharp change of the transport properties reflects such an instability of the electronic state. The charge ordering reduces the density of states at the Fermi level and suppresses the superconductivity. The connection between the appearance of negative thermopower and the suppression of superconductivity can be interpreted naturally by this picture.

Acknowledgements

I would like to express my sincere appreciations to Professor Toshizo Fujita and Associate Professor Yoshiteru Maeno for their useful guidance, strong encouragement, valuable advice and critical reading of this thesis. I wish to thank Dr.Takashi Suzuki and Fumihiko Nakamura for fruitful discussion and useful advice. I am particularly grateful to Dr.Koji Yoshida, Mr.Yasuki Tanaka and Jørgen Nyhus for their help in experiments during a long time. I am also indebted to all of the students of our group for their friendly sentiments. I would like to thank all members of the Department of Physics for their hospitalities during the years I study in Hiroshima University.

References

[1] A.R. Moodenbaugh, Y. Xu, M. Suenaga, T.J. Folkerts and R. N. Shelton, Phys. Rev. B **38** (1988) 4596.

[2] Both abbreviations THT and HTT for the tetragonal phase at high temperatures have been widely used at least since mid 1970's in the study of organic K_2NiF_4-type compounds. In light of the orthorhombic phase at low temperatures found later in Nd-substituted $La_{2-x}Sr_xCuO_4$, we much prefer to place O (for orthorhombic, or T for tetragonal) in front and designate Bmab and Pccn phases as OMT (mid-temperature orthorhombic) and OLT (low-temperature orthorhombic), respectively. Some authors use LTO (low temperature orthorhombic) and LTLO (low temperature less orthorhombic) for these phases.

[3] J.D. Axe, D. E. Cox, K. Mohanty, H. Moudden, A. R. Moodenbaugh, Y. Ku and Y. R. Thurston, IBM J. Res Develop. **33** (1989) 382.

[4] T. Suzuki and T. Fujita, J. Phys. Soc. Jpn. **58** (1989) 1883; Physica C **159** (1989) 111.

[5] J.D. Axe, A.H. Moudden, D. Hohlwein, D.E. Cox, K.M. Mohanty, A.R. Moodenbaugh, and Y.W. Xu, Phys. Rev. Lett. **62** (1989) 2751.

[6] K. Yoshida, F. Nakamura, Y. Tanaka, Y. Maeno and T. Fujita, Physica C **203** (1994) 371.

[7] Y. Maeno, N. Kakehi, M. Kato and T. Fujita, Phys. Rev. B **44** (1991) 7753.

[8] Y. Maeno, F. Nakamura, T. Suzuki and T. Fujita, JJAP series **7** "Mechanisms of Superconductivity" (1992) 91.

[9] X.Z. Bao, Y. Maeno, Y. Tanaka, K. Yoshida and T. Fujita, Advances in the Superconductivity **VI** (1994) 375.

[10] Y. Koike, T. Kawaguchi, N. Watanabe, T. Noji, and Y. Saito, Solid State Commun. **79** (1991) 155.

[11] X.Z. Bao, Y. Maeno, F.Nakamura, S. Nishizaki and T. Fujita, Advances in

Superconductivity **VII** (1995) 241.

[12] M.K. Crawford, R.L. Harlow, E.M. McCarron, W.E. Farneth, J.D. Axe, H. Chou and Q.Huang, Phys. Rev. B **44** (1991) 7749.

[13] B. Büchner, M. Cramm, M. Braden, W. Braunisch, O. Hoffels, W. Schnelle, R. Müller, A. Freimuth, W. Schlabitz, G. Heger, D.I. Khomskii and D. Wohlleben, Europhys. Lett. **21** (1993) 953.

[14] S.J.L. Billinge, G.H. Kwei, A.C. Lawson, J.D. Thompson and H. Takagi, Phys. Rev. Lett. **71** (1993) 1903.

[15] B. Büchner, M. Breuer and A. Freimuth, Phys. Rev. Lett. **73**(1994)1841.

[16] F. Nakamura, K. Yoshida, Y. Tanaka, X.Z. Bao, Y. Maeno and T. Fujita, J. Supercon. **7** (1994) 33.

[17] N. Yamada and M. Ido, Physica C **203** (1992) 240.

[18] S. Katano, S. Funahashi, N. Môri, Y. Ueda and J.A. Fernandez–Baca, Phys. Rev. B **48** (1993) 6549.

[19] Y. Tanaka, Y. Maeno, F. Nakamura and T. Fujita, Physica B **194–196** (1994) 2053.

[20] J. Yamada, M. Sera, M. Sato, T. Takayama, M. Takata and M. Sakata, J. Phys. Soc. Jpn. **63** (1994) 2314.

[21] R.P. Reed and A.F. Clark, Materials at Low Temperatures (American Society of Metals, Ohio, 1993).

[22] D.K.C. MacDonald, Thermoelectricity (John Wiley & Sons, New York, 1962).

[23] T. Suzuki, M. Sera, T. Hanaguri and T. Fukase, Phys. Rev. B **49** (1994) 12392.

[24] R.D. Barnard, Thermoelectricity in metals and alloys (Taylor & Francis, London, 1972).

[25] J.T. Chen, C.J. McEwan, L.E. Wenger and E.M. Logothetis: Phys. Rev. B **35** (1987) 7124.

[26] J.R. Cooper, B. Alavi, L–W. Zhou, W.P. Beyermann and G. Grüner, Phys. Rev. B **35** (1987) 8794.

[27] M.F. Hundley, A. Zettl, A. Slacy and Marvin L. Cohen, Phys. Rev. B **35** (1987) 8800.

[28] C. Uher, A.B. Kaiser, E. Gmelin and L. Walz, Phys. Rev. B **36** (1987) 5676.

[29] R.C. Yu, M.J. Naughton, X. Yan, P.M. Chaikin, F. Holtzberg, R.L. Greene, J. Stuart and P. Davies, Phys. Rev. B **37** (1988) 7963.

[30] M. Sera, Y. Ando, S. Kondoh, K. Fukuda, M. Sato, I. Watanabe, S. Nakashima and K. Kumagai, Solid State Commun. **69** (1989) 851.

[31] Y. Nakamura and S. Uchida, Phys. rev. B **46** (1992) 5841

[32] M. Sera, T. Nishikawa and M. Sato, J. Phys. Soc. Jpn. **62** (1993) 281.

[33] J. Takeda, T. Nishikawa and M. Sato, Physica C **231** (1994) 293.

[34] T. Suzuki, M. Sera and T. Fukase, Physica C **235–240** (1994) 1315.

[35] N. Mitra, J. Trefny, M. Young and B. Yarar, Phys. Rev. B **36** (1987) 5581.

[36] C. Uher, A.B. Kaiser, E. Gmelin and L. Walz, Phys. Rev. B **36** (1987) 5676.

[37] U. Gottwick, R. Held, G. Sparn, F. Steglish, H. Rietschel, D. Ewert, B. Renker, W. Bauhofer, S. von Molnar, M. Wilhelm and H.E. Hoenig, Europhys. Lett.,**4** (10), (1987)1183.

[38] H.J. Trosahl and A. Mawdsley, Phys. Rev. B **36** (1987) 8881.

[39] S.C. Lee, J.H. Lee, B.J. Suh,S.H. Moon, C.J. Lim and Z.G. Khim, Phys. Rev. B **37** (1988) 2285.

[40] A.P. Goncalves, I.C. Santus, E.B. Lopes, R.T. Henriques, M. Almeida and M.O. Figueiredo, Phys. Rev. B **37** (1988) 7476.

[41] J. Clayhold, S. Hagen, Z.Z. Wang, N.P. Ong, J.M. Tarascon and P. Barboux, Phys. Rev. B **39** (1989) 777.

[42] W.N. Kang, K.C. Cho, Y.M. Kim and M.Y. Choi, Phys. Rev. B **39** (1989) 2763.

[43] A.B. Kaiser and G. Mountjoy, Phys. Rev. B **43** (1991) 6266.

[44] J.L. Cohn, E.F. Skelton, S.A. Wolf and J.Z. Liu, Phys. Rev. B **45** (1992) 13140.

[45] S.D. Oberlelli, J.R. Cooper and J.L. Tallon, Phys. Rev. B **46** (1992) 14928.

[46] J.R. Cooper and A. Carrington, Advances in Superconductivity **V** (1993) 95.

[47] J.W. Cochrane, G.J. Russell and D.N. Matthews, Physica C **232** (1994) 89.

[48] P.M. Chaikin and G. Beni, Phys. Rev. B **13** (1976) 647.

[49] J.F. Kwak and G. Beni, Phys. Rev. B **13** (1976) 652.

[50] H.J. Trodahl, Phys. Rev. B **51** (1995) 6175.

[51] S. Sakita, T. Suzuki, F. Nakamura, M. Nohara Y. Maeno and T.Fujita, Physica B **219 & 210** (1996) 216.

[52] K. Ito, Y. Koyama, Y. Wakabayashi, and Y. Inoue, Advances in Superconductivity **VIII** (1996) 239.

[53] J.M. Tranquada, B.J. Sternlieb, J.D. Axe, Y. Nakamura and S. Uchida, Nature **375** (1995) 561.

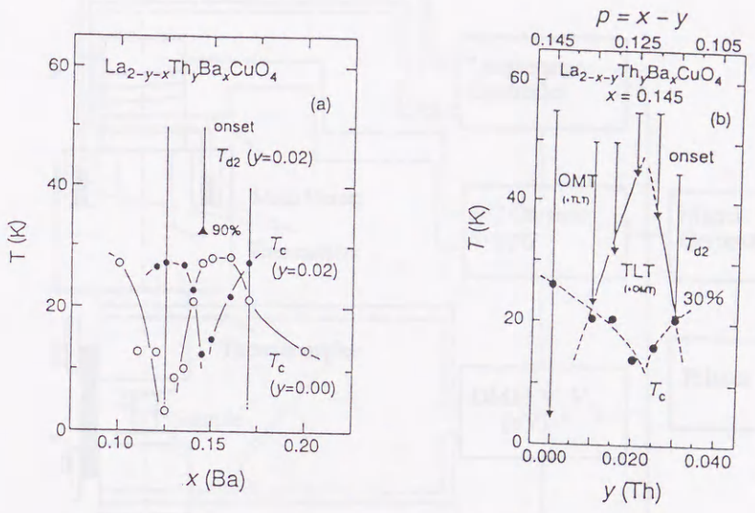

Fig. 1. Superconductivity transition temperature T_c and the low-temperature structural phase transition temperature T_{d2} of Th-substituted $La_{2-x}Ba_xCuO_4$. $p = x - y = 0.125$, is the essential condition which leads to the low-temperature anomalies in $La_{2-x-y}Th_yBa_xCuO_4$ as functions of both x and y. T_c is defined at the temperature at witch the sample is of 1% volume fraction of perfect diamagnetism. T_{d2} is defined as the temperature at which the integrated intensity ratio of the TLT phase becomes 90% in Fig.1(a) and 30% in Fig.1(b).

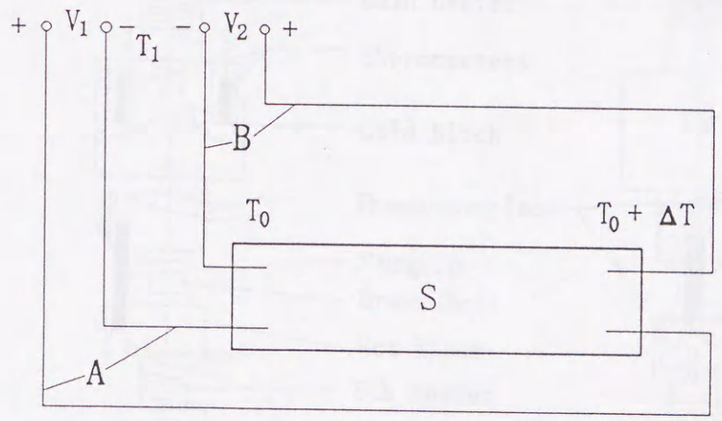

fig. 2. Experiment principle for thermopower. S: sample, A: copper, B: constantan. The thermopower of the sample at given temperature can be attained by measuring V_1 and V_2.

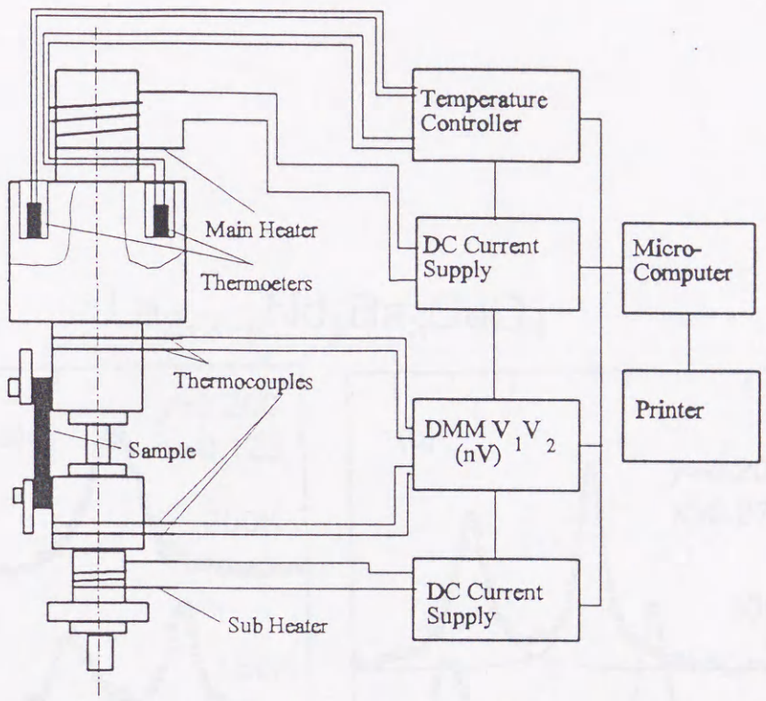

Fig. 3. General layout of the setup for the measurement of thermopower.

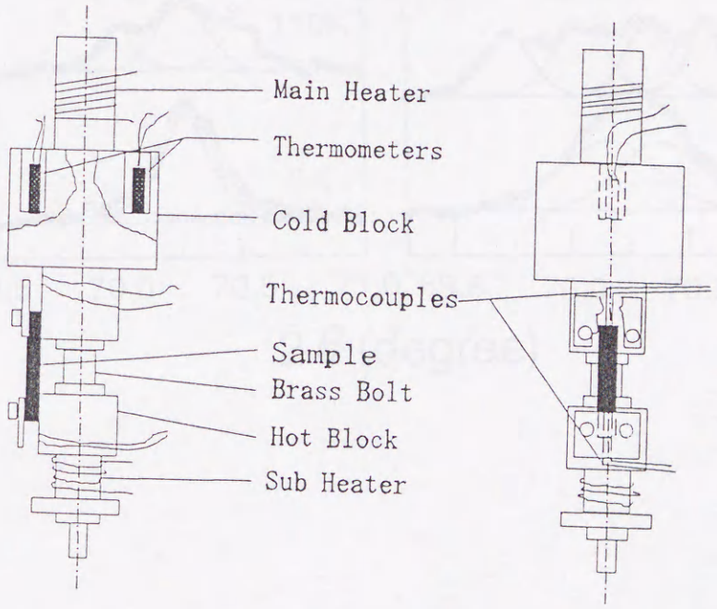

Fig. 4. Sample holder for the measurement of thermopower.

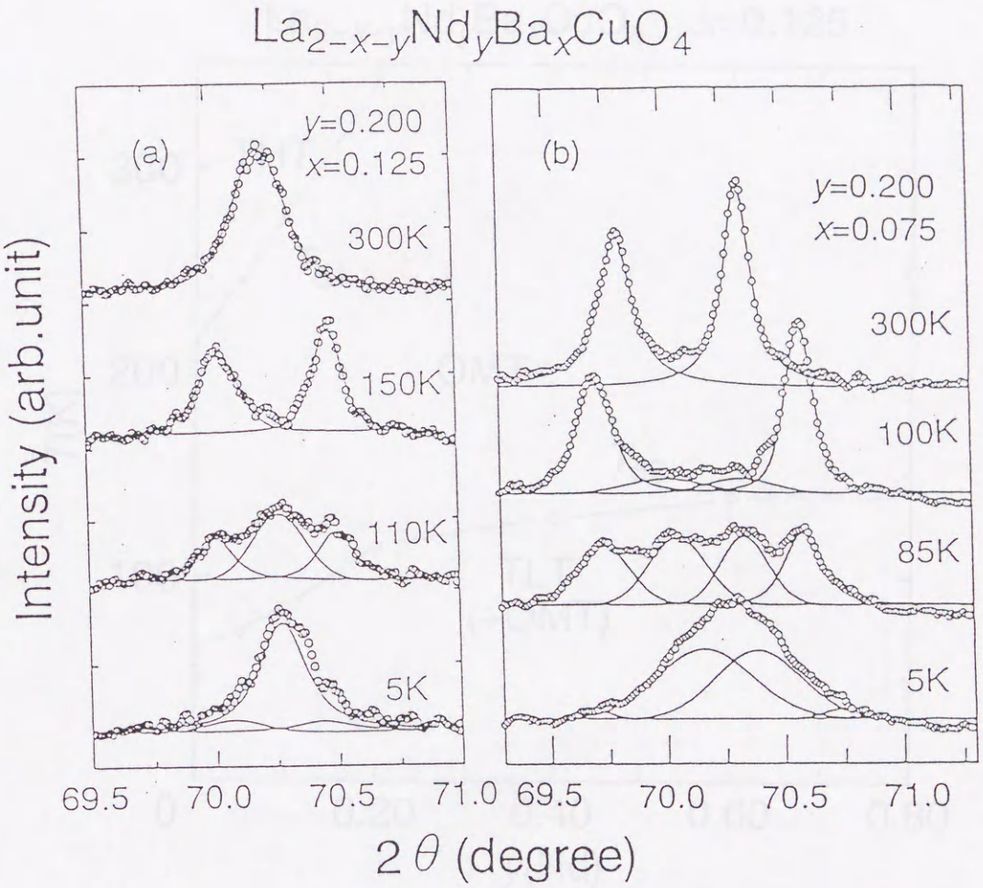

Fig. 5. Powder X-ray diffraction spectra of $La_{2-x-y}Nd_yBa_xCuO_4$ with (a) x=1/8, y=0.20 and (b) x=0.075, y=0.20 at selected temperatures. Circles represent the data points and solid curves indicate the results of multiple-peak fittings.

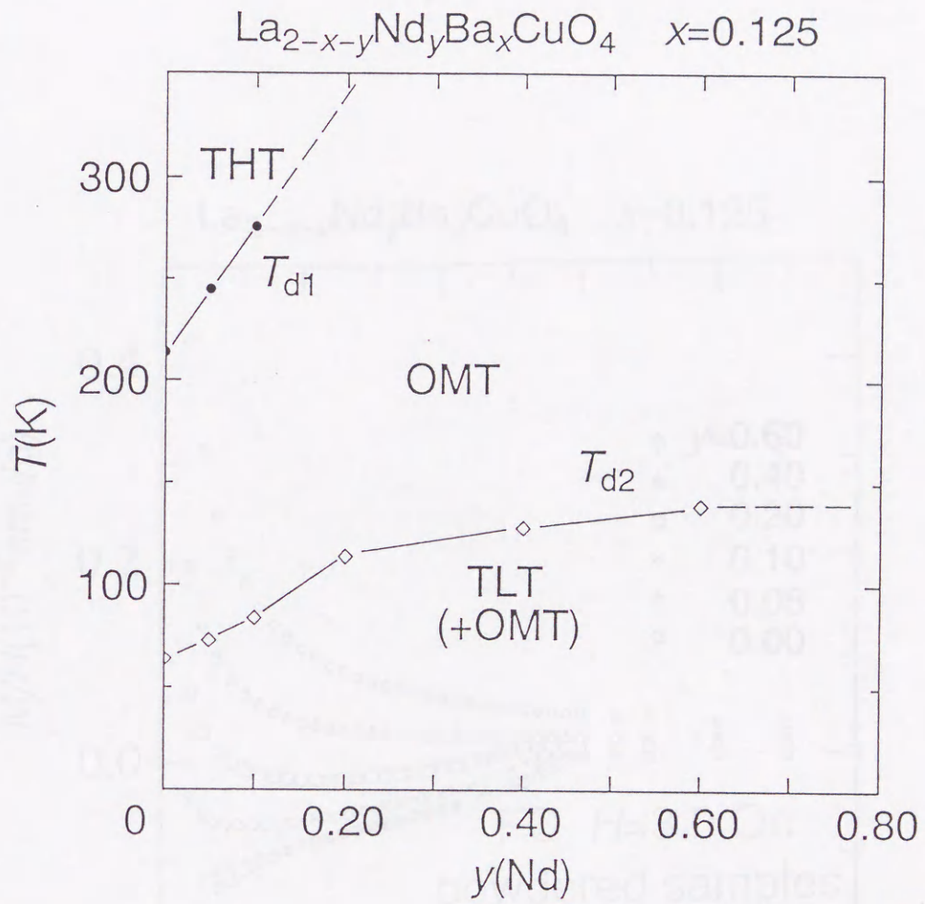

Fig. 6. Nd concentration dependence of T_{d1} (●) and T_{d2} (◇). T_{d2} is defined as the temperature at which the integrated intensity ratio of the TLT phase becomes 50%.

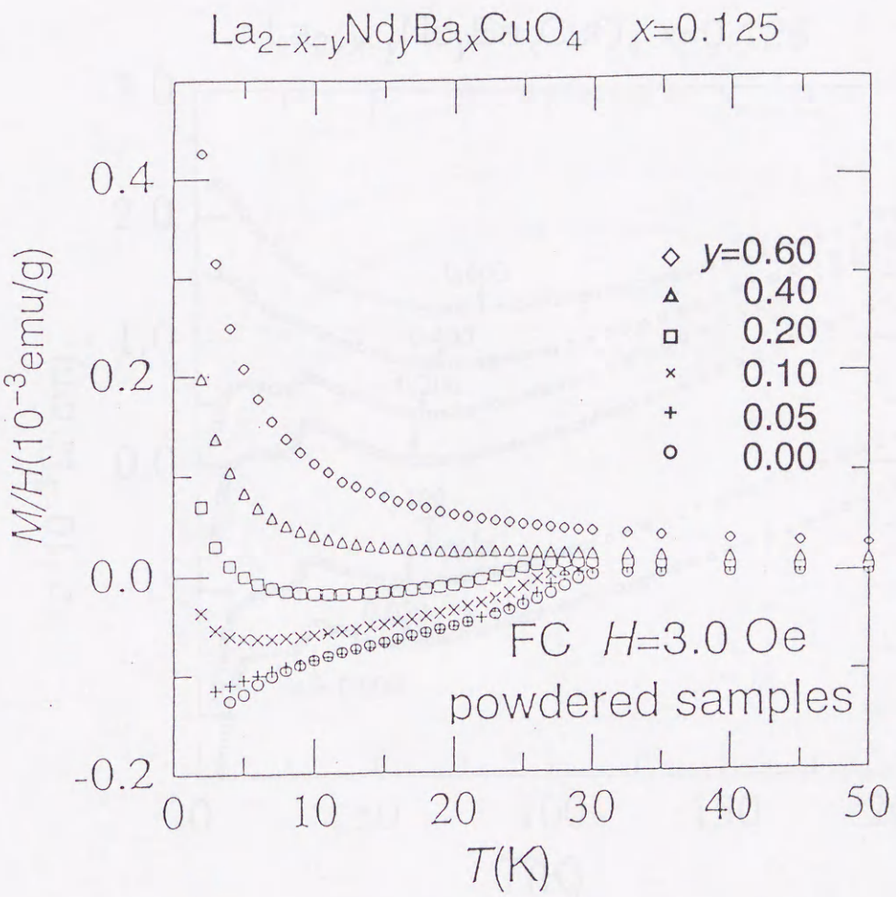

Fig. 7. Magnetization of powdered samples of $La_{2-x-y}Nd_yBa_xCuO_4$ (x=1/8) measured by a SQUID magnetometer on cooling in a field of 3.0 Oe.

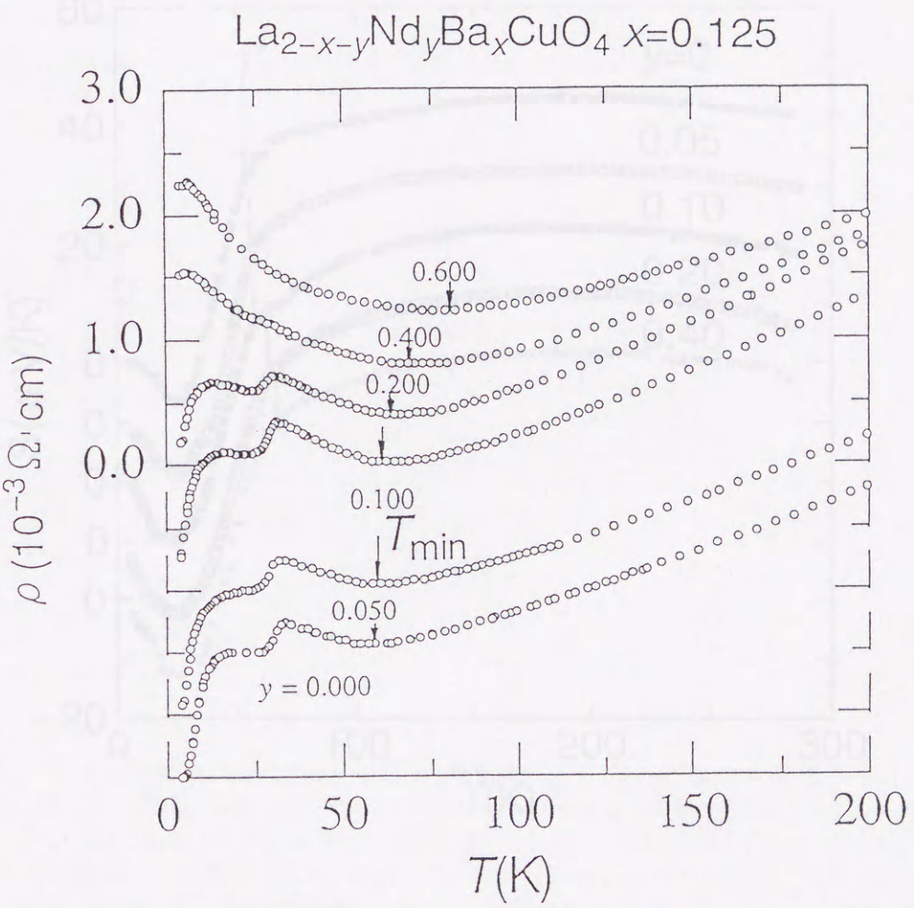

Fig. 8. Variation of the resistivity with temperature, showing a distinctive upturn below T_{min}=60–70K. There is no anomaly in the resistivity at T_{d2}.

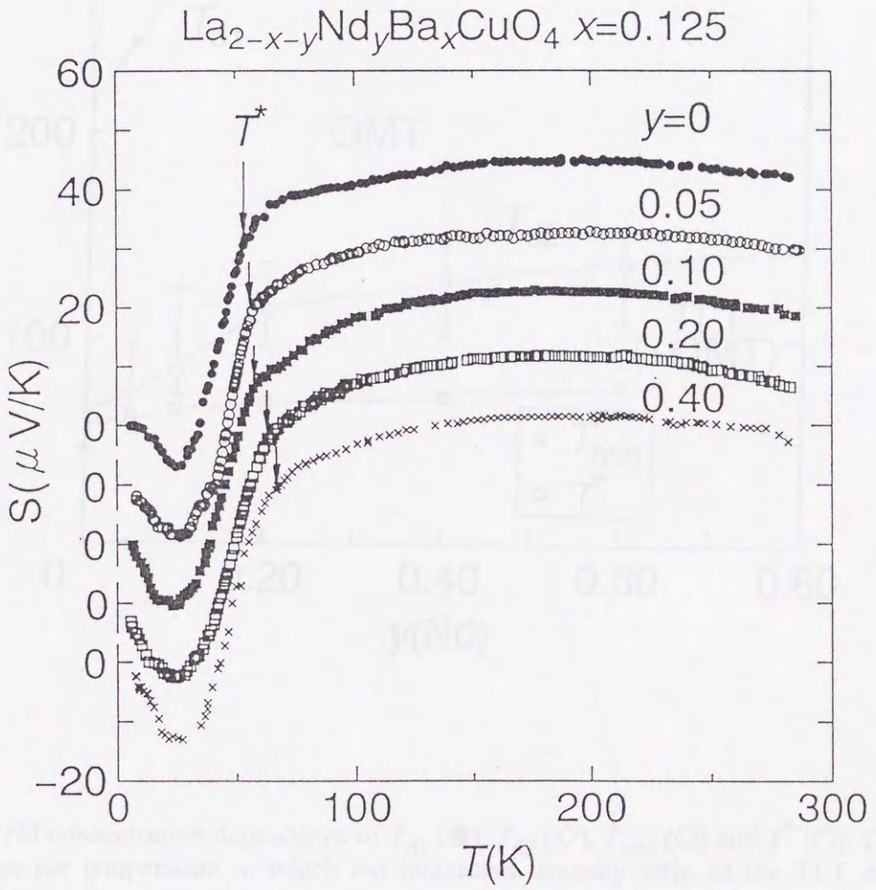

Fig. 9. Temperature dependence of the thermopower $S(T)$. A sharp change of the thermopower is observed at T^*=60–70K, below which $S(T)$ decreases rapidly towards negative values. There is no anomaly in the thermopower at T_{d2}.

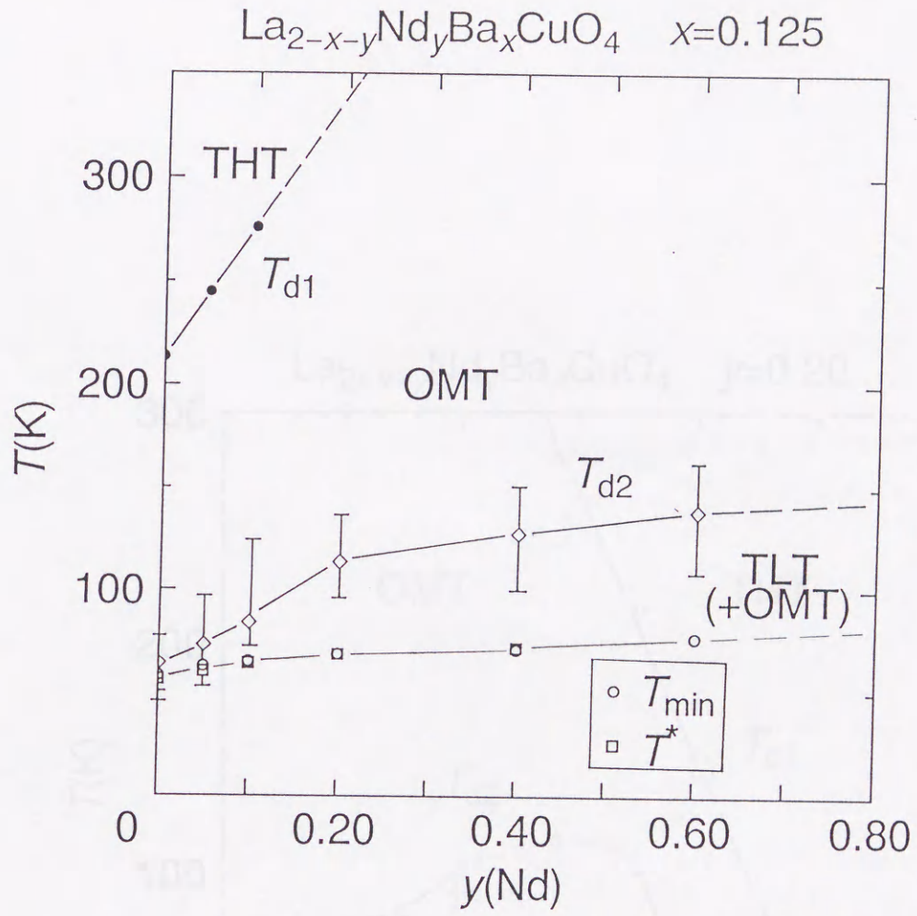

Fig. 10. Nd concentration dependence of T_{d1} (●), T_{d2} (◇), T_{min} (○) and T^* (□). T_{d2} is defined as the temperature at which the integrated intensity ratio of the TLT phase becomes 50%. Top ends of the vertical bars represent the onset of the structural phase transition, and bottom ends the temperature at which the intensity of the TLT peaks begins to saturate. For a given Nd concentration, the values of T_{min} and T^* are nearly the same but the value of T_{d2} is higher than those of T_{min} and T^* for the samples with higher Nd concentration.

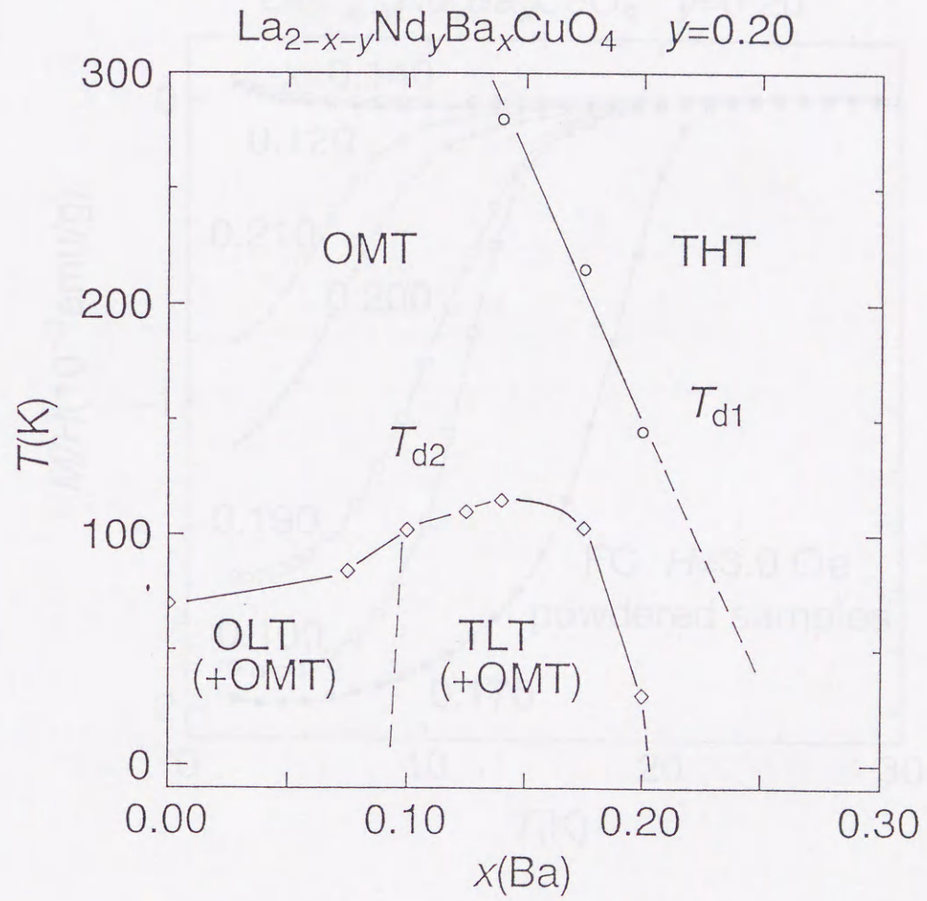

Fig. 11. Ba concentration dependence of T_{d1} and T_{d2} for $La_{2-x-y}Nd_yBa_xCuO_4$ (y=0.20).

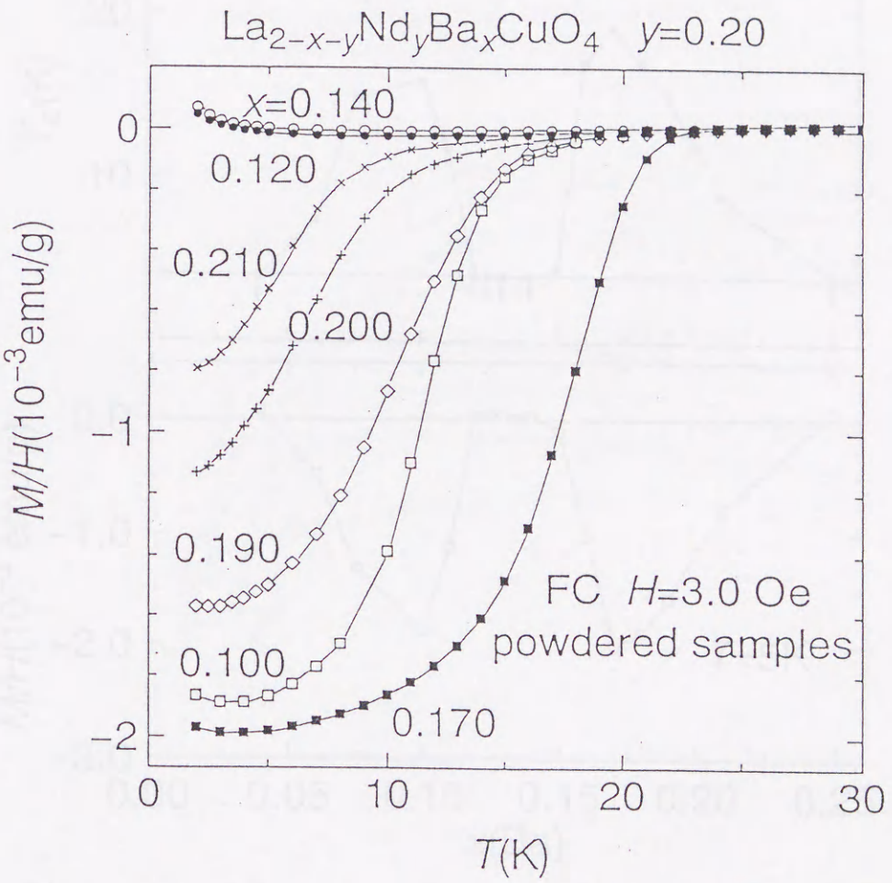

Fig. 12. Magnetization of powdered samples of $La_{2-x-y}Nd_yBa_xCuO_4$ (y=0.20) measured by a SQUID magnetometer on cooling in a field of 3.0 Oe.

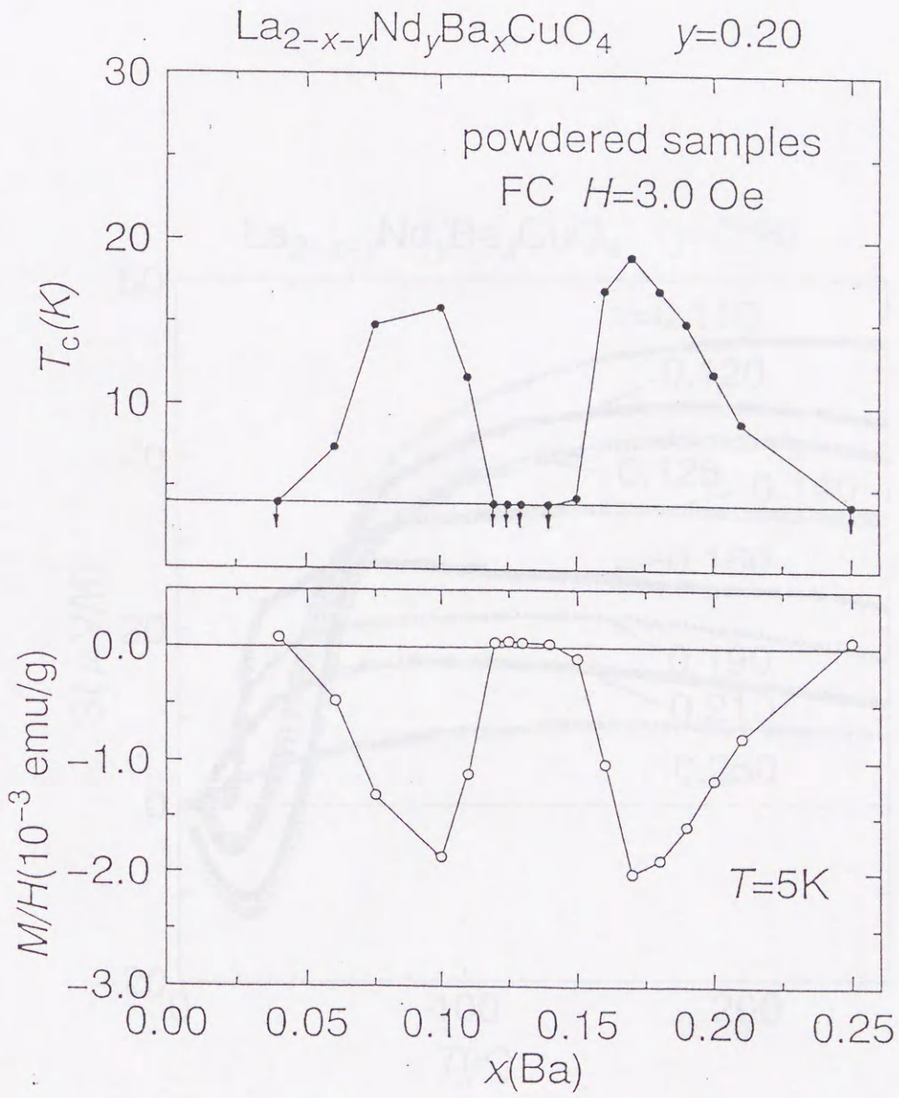

Fig. 13. Ba concentration dependence of T_c and magnetic susceptibility at 5K. T_c is defined as the temperature at which a sample exhibits 1% volume fraction of perfect diamagnetism.

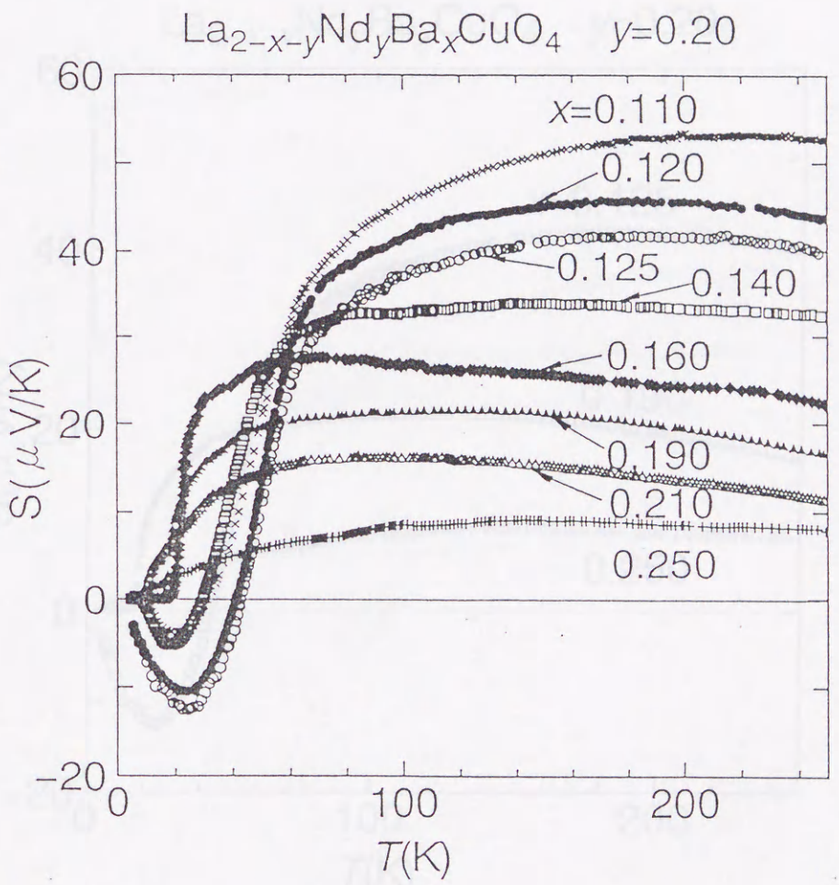

Fig. 14. Temperature dependence of the thermopower of $La_{2-x-y}Nd_yBa_xCuO_4$ (y=0.20)

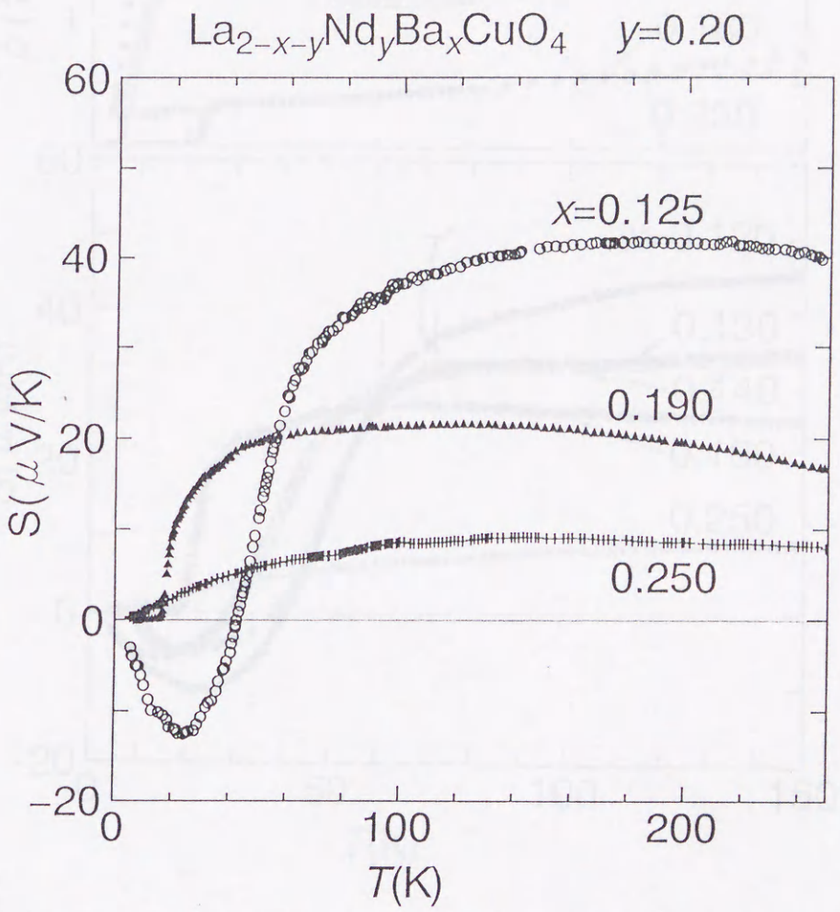

Fig. 15. At lower temperatures $S(T)$ approaches zero in three kinds of ways depending on x for the samples of $La_{2-x-y}Nd_yBa_xCuO_4$ (y=0.20).

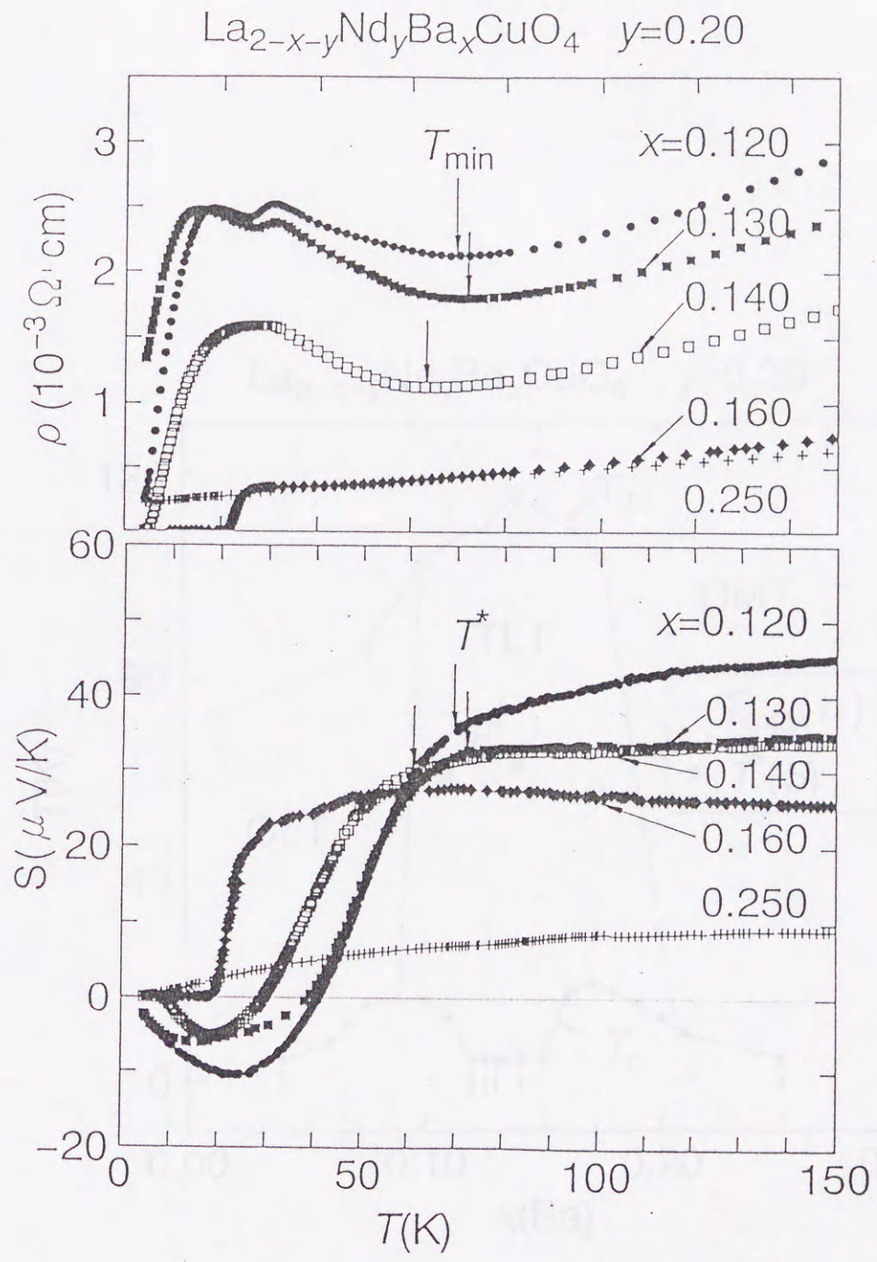

Fig. 16. Relationship between the anomaly of resistivity and that of thermopower. For the same Ba concentration the values of T_{min} and T^* are nearly the same with x around 1/8. T_{min} is defined as the temperature at which the resistivity of the sample takes a minimum. T^* is defined as the temperature at which the thermopower begins to fall down sharply.

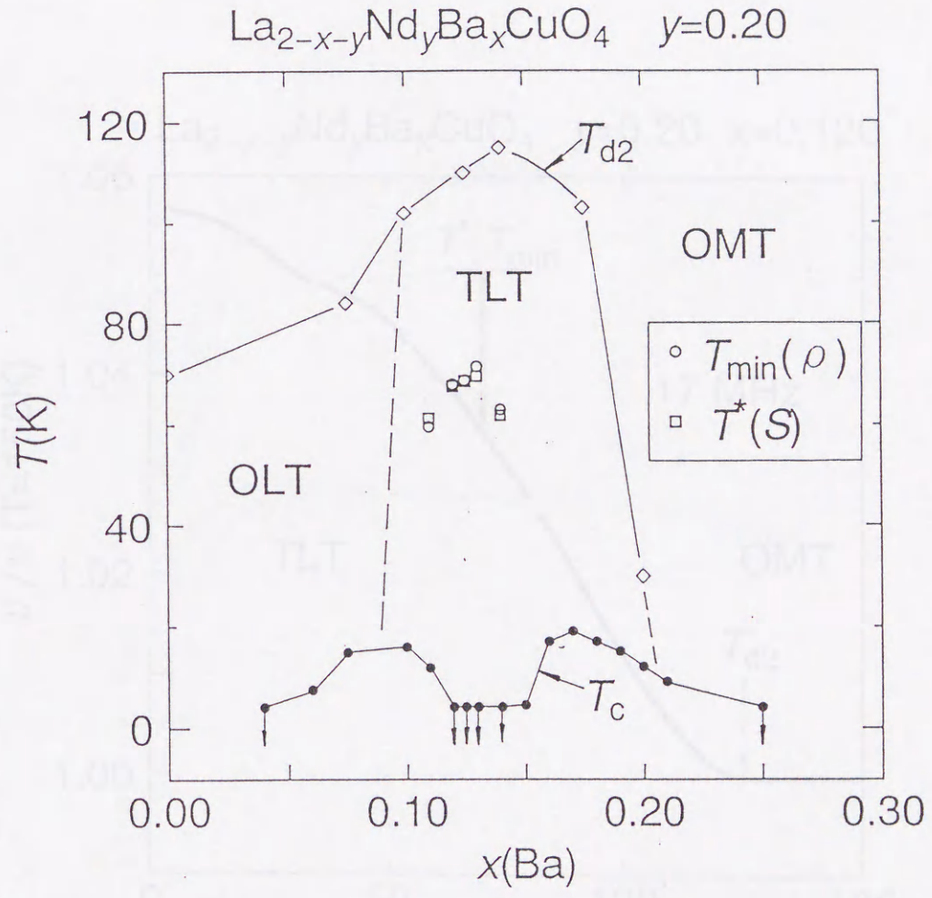

Fig. 17. Ba concentration dependence of T_c (●), T_{d2} (◇), T_{min} (○) and T^* (□). For the same Ba concentration, the values of T_{min} and T^* are nearly the same but the value of T_{d2} is about 50K higher than those of T_{min} and T^*.

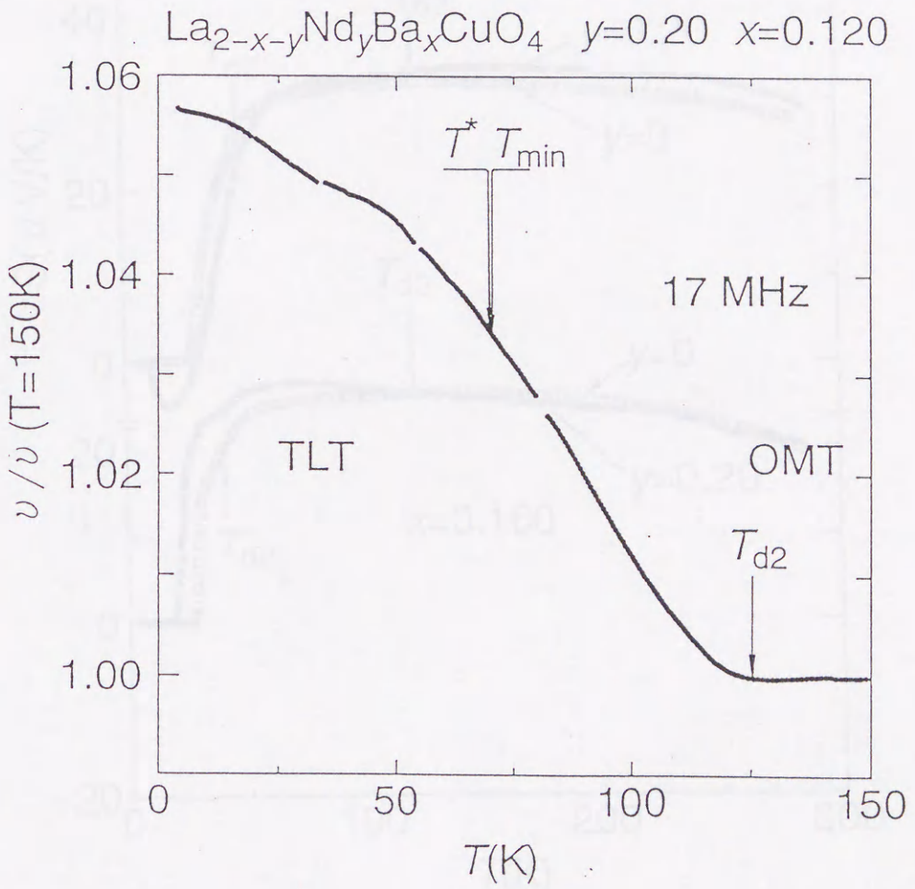

Fig. 18. Temperature dependence of the ultrasonic velocity of LNBCO with x=0.120 and y=0.20. At T_{min} and T^* there is no anomaly in this curve.

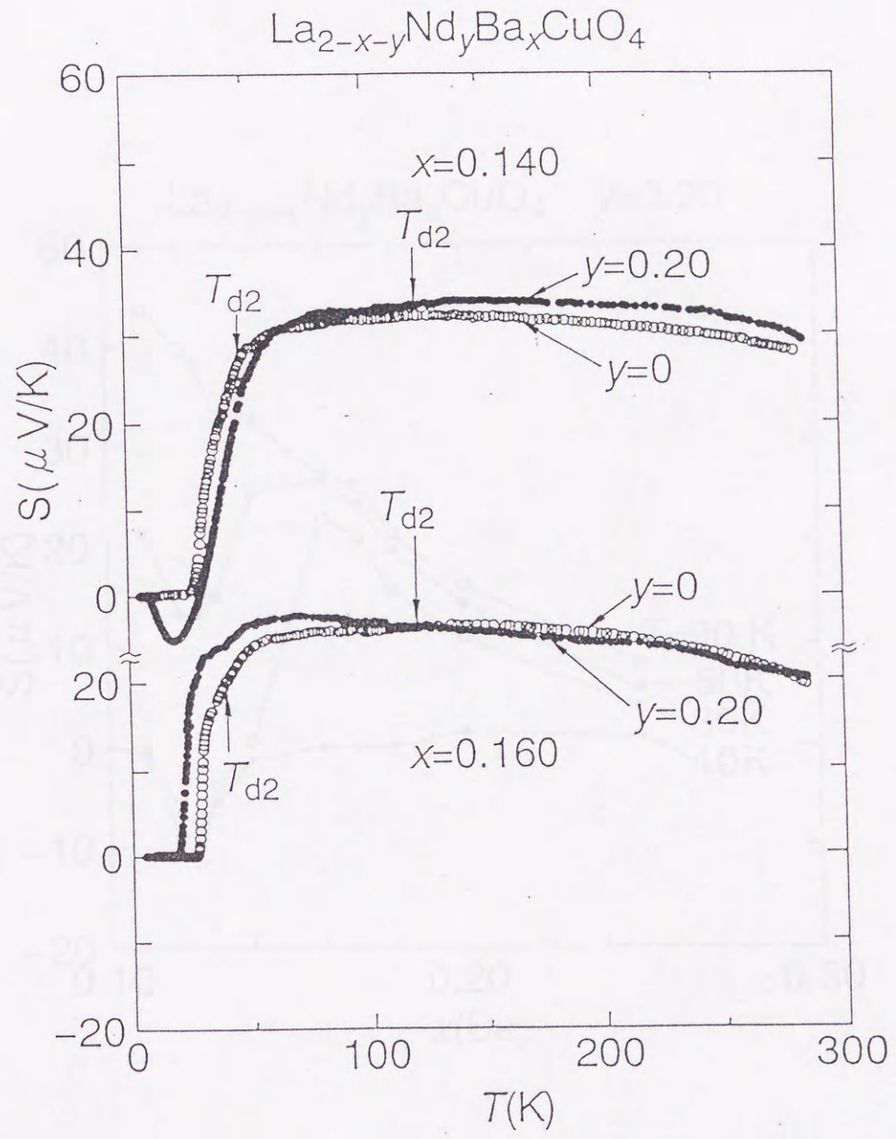

Fig. 19. Comparison of thermopower between LBCO (y=0) and LNBCO (y=0.20).

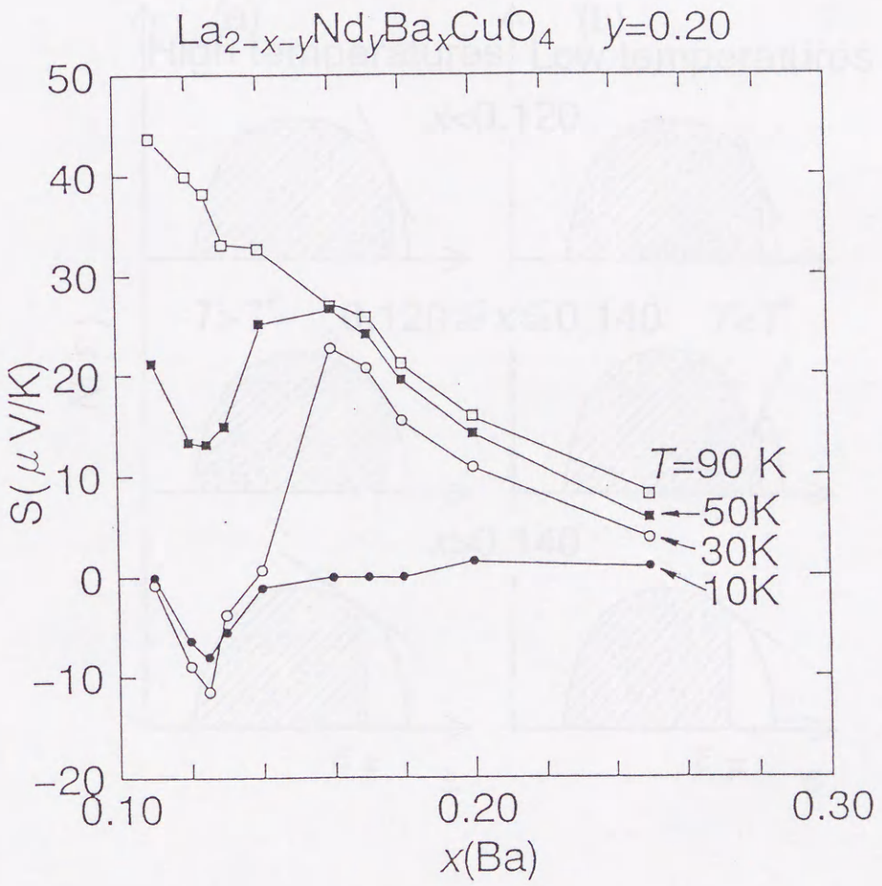

Fig. 20. Ba concentration dependence of thermopower at selected temperatures.

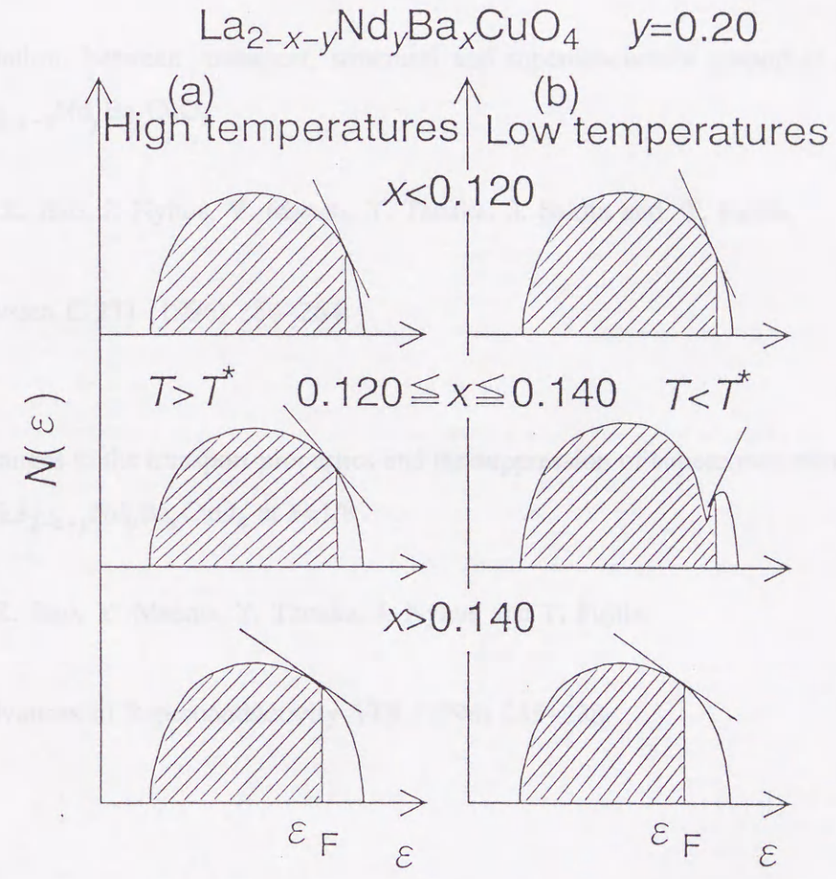

Fig. 21. A simple model of the density of states for $x<1/8$, $x\approx1/8$ and $x>1/8$. (a) at high temperatures (b) at low temperatures.

公表論文

[1] Relation between transport, structural and superconductive properties in $La_{2-x-y}Nd_yBa_xCuO_4$

X. Z. Bao, J. Nyhus, Y. Maeno, Y. Tanaka, S. Sakita and T. Fujita,

Physica C **271** (1996) 256–264.

[2] Changes in the transport properties and the suppression of superconductivity in $La_{2-x-y}Nd_yBa_xCuO_4$ at x=1/8

X.Z. Bao, Y. Maeno, Y. Tanaka, J. Nyhus and T. Fujita,

Advances in Superconductivity **VIII** (1996) 235–238.

参考論文

[1] Superconductivity and Structural Phase Transition in $La_{2-x}Ba_xCuO_4$ with La Partially Replaced by Th

X.Z. Bao, Y. Maeno, Y. Tanaka, K. Yoshida and T. Fujita,

Advances in Superconductivity **VI** (1994) 375–378.

[2] Effect of Tb Substitution on the Superconductivity of $La_{2-x}Ba_xCuO_4$

X.Z. Bao, Y. Maeno, F. Nakamura, S. Nishizaki and T. Fujita,

Advances in Superconductivity **VII** (1995) 241–244.

[3] Stability of the low-temperature tetragonal phase in $La_{2-x}Ba_xCuO_4$ and related compounds

F. Nakamura, K. Yoshida, Y. Tanaka, X.Z. Bao, Y. Maeno and T. Fujita

J. Supercon. **7** (1994) 33–35.